

Optical and Electrical Properties of Solvothermally Synthesized Manganese Doped Cuprous Oxide Nanoparticles

A Suganthi*¹, S John Kennady Vethanathan², S Perumal³, D Priscilla Koilpillai²
S Karpagavalli¹

*¹Department of Physics, Govindammal Aditanar College for women, M.S. University, Tamilnadu.

²Department of Physics, St. John's College, M.S. University, Tamilnadu.

³Department of Physics, Noorul Islam college of arts and science, M.S. University, Tamilnadu.

Abstract: Manganese doped Cuprous Oxide Nanoparticles were synthesized by facile solvothermal scheme without any surfactants or templates. The structural, optical and electrical properties of the samples were investigated using X-ray diffraction (XRD), Fourier Transform Infrared (FTIR) spectroscopy, Ultraviolet-Visible spectroscopy, Scanning electron microscopy (SEM), Energy dispersive X-ray analysis (EDAX) and impedance spectroscopy measurements. XRD analysis revealed that Manganese doped cuprous oxide nanoparticles were formed in good crystalline quality. The grain size of the nanoparticles was found to be in range of 41 ~33nm. SEM image indicated that the synthesized nanoparticles exhibit flower like structure. The presences of the compositions were confirmed from the EDAX analysis. UV-Visible absorption spectra showed that the band transition is around 278 nm. Impedance spectroscopy was employed to study the electrical resistance versus frequency.

Keywords: Crystalline, domine, grain, Solvothermal, XRD.

I. Introduction

In recent years, fabrication and characterization of nanostructured metal oxide materials have been considered a cornerstone in materials science for both fundamental as well as technological reasons [1-4]. Among various transition metal oxides Cu₂O has attracted much attention due to its fascinating properties. It is a prospective candidate for low cost photovoltaic applications due to its high optical absorption coefficient, lower band gap energy and for nontoxic and large abundance of the base material copper. It is also an ideal compound using as a dilute magnetic semiconductor (DMS). It has been used as heterogeneous catalysts in many important chemical processes and oxidation of carbon monoxide, hydrocarbon and phenol in super critical water [5]. Various methods are used to prepare nanoparticles of copper oxides, including sol-gel, precipitation-stripping, solid-state reaction, alkoxide based synthesis, precipitation-pyrolysis and thermal decomposition [6-14]. Among these techniques for the synthesis of copper oxide nanoparticles, solvothermal process is a novel method; it is much faster and more economical [15]. In this report, we have synthesized Manganese doped Cu₂O nanoparticles using a simple and low cost microwave irradiation process. The aim of this paper is to evaluate the changes in the structural, morphological, optical and electrical properties of copper nanoparticles brought about through successful doping with Manganese (2wt%, 4 wt%, 6wt% & 8 wt %).

II. Materials and Methods

All the chemical reagents used in these experiments are analytical grade and were used without further purification. Copper acetate and urea are taken as solute in the molecular ratio 1:3 and dissolved in 100 ml ethylene glycol individually. The solutions are mixed together. The prepared solution is kept in a domestic microwave oven (frequency 2450MHz & power 900 Watt). Microwave irradiation is carried out for 10-20 minutes till the solvent is evaporated completely. The obtained colloidal precipitate is washed with distilled water and acetone. The prepared sample is dried in atmospheric air. For Manganese doping, Manganese acetate (2wt%, 4 wt%, 6wt% & 8 wt %) are added with the above precursors and the same procedure was repeated.

III. Structural Characterization

3.1. XRD Analysis:

In order to confirm the materials of the grown particles and to determine the particle size, powder X-ray diffraction (PXRD) data were collected for all the three samples prepared using an automated X-ray powder diffractometer with CuK α radiation ($\lambda=1.5406\text{\AA}$). Using the observed 2θ (Bragg angle) and d (interplanar spacing) all the reflections were indexed. The PXRD patterns of Manganese doped samples were shown in Fig.1

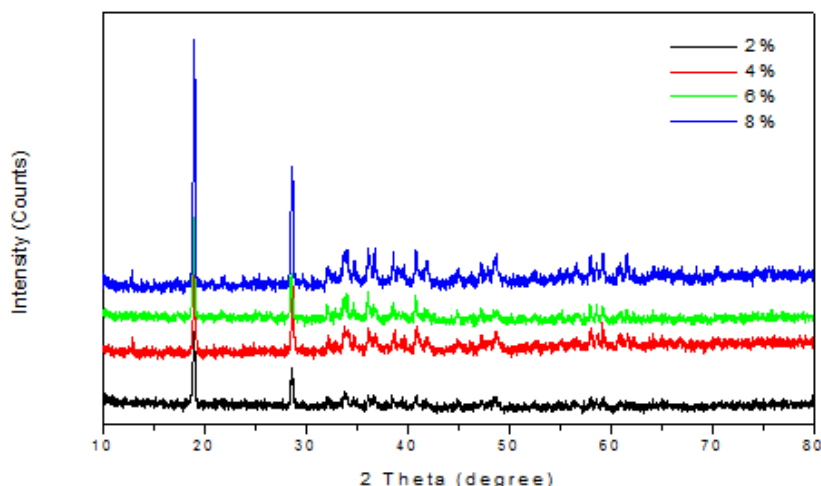


Figure.1. XRD patterns of Mn doped Cu₂O Nanoparticles

Mn doped Cu₂O nanoparticles belong to the cubic lattice system. All diffraction peaks can be indexed in the Cu₂O cubic structure, which was confirmed from the ICDD card no (78-2076). The planes (110), (111), (200), (220), (311) and (222) are corresponding to Cu₂O nanoparticles. No peaks of impurities are found in XRD pattern. The XRD data confirms that addition of dopant in Cu₂O lattice does not alter its lattice, but it produces slight shift in diffraction peaks. It confirms the incorporation of dopant in host lattice. The ionic radius of Mn⁺³ (0.58Å⁰) is smaller than that of Cu⁺² (0.73Å⁰) that is why crystallite size decreases for higher doping concentration. Calculated crystallite size (Using Debye scherre’s equation), lattice parameters and cell volume of the prepared particles was given in table 1.

Table 1. Variation Of Crystallite Size & Lattice Constants With Dopant Concentration

Dopant Concentration (%)	Crystallite Size (nm)	Lattice Parameters (Å ⁰) a=b=c	Cell Volume (Å ³)
2	41	4.3131	80.236
4	38	4.3114	80.142
6	35	4.3171	80.461
8	33	4.3175	80.482

3.2. SEM analysis:

The morphology of the prepared powders was examined by SEM (Fig. 2). The average size of the image was found out using Image J software. Mn doped Cu₂O nanoparticles exhibit rose flower like structure [16, 17].

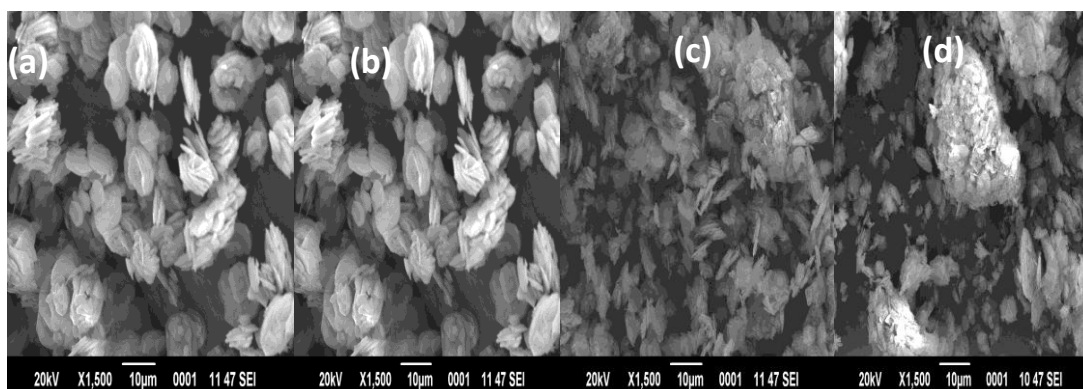


Figure.2. SEM images of Mn doped Cu₂O nanoparticles: (a) 2%, (b) 4%, (c) 6% and (d) 8%

3.3. EDAX analysis:

The presence of Mn in doped samples was confirmed from the selective area EDAX analysis. EDAX spectra of Mn doped Cu₂O is shown in Fig 3. From figure we know that Mn was successfully incorporated in the system.

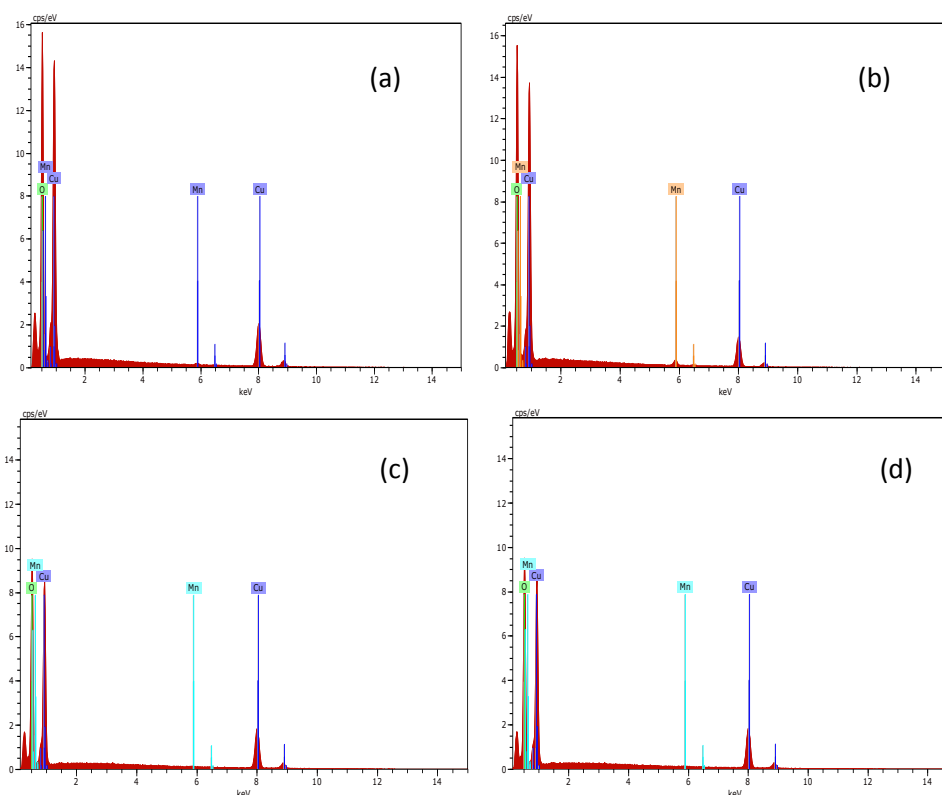


Figure3. EDAX spectra of Mn doped Cu₂O nanoparticles: (a) 2%, (b) 4%, (c) 6% and (d) 8%

3.4. FTIR Analysis:

The composition and quality of the products were analysed by FTIR. The analysis was performed by SHIMADZU MODEL-IRAFFINITY-1. Fig 4 shows the typical FTIR spectra of the samples.

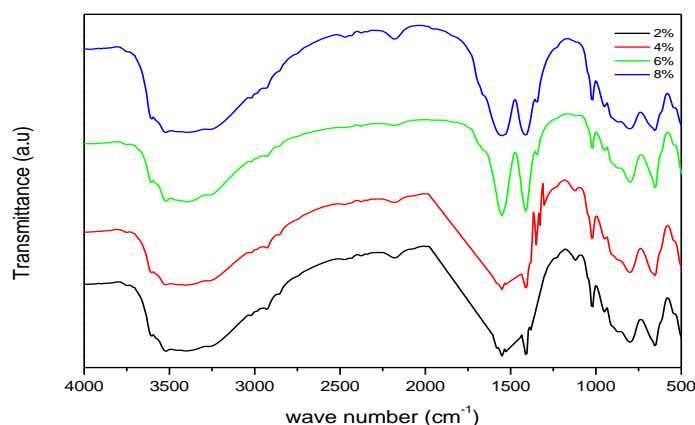


Figure.4. FTIR spectra of Mn (2%, 4%, 6% & 8%) doped Cu₂O Nanoparticles

The peak at 3500cm⁻¹ and 1624cm⁻¹ represents (O-H) water tensional tremble. The peak at 2362cm⁻¹ is attributed to C-H tensional. The peak at 1458cm⁻¹ and 1384cm⁻¹ represents (N-O) and (C-O) tremble respectively. The peak at 986cm⁻¹ represents (O-C-O) tensional tremble and 608 cm⁻¹ reveals the dopant Mn-O tremble respectively.

IV. Optical Characterization

UV-Visible absorption spectroscopy has been used to investigate the optical properties of Mn doped Cu₂O nanoparticles. UV-Visible absorption spectra of as synthesized Mn doped Cu₂O nanoparticles have been recorded by UV-Visible spectrophotometer in the wavelength range of 250nm to 1000nm. The spectrum is shown in Fig 5.

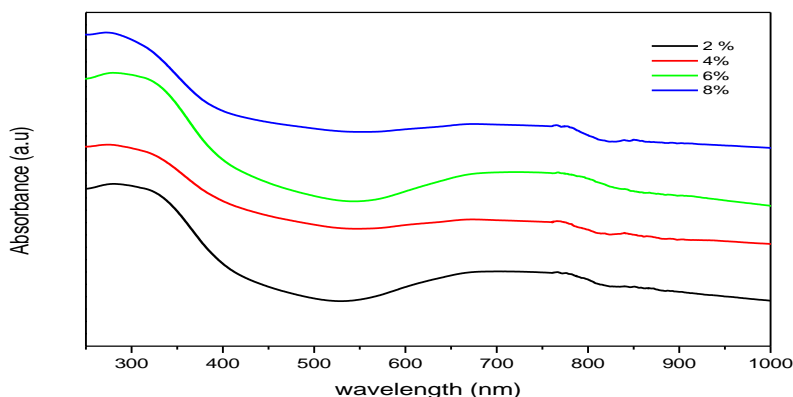


Figure 5. UV-Visible spectrum of Mn doped Cu₂O Nanoparticles

The samples exhibit an absorption edges at 283, 275, 273 & 264 nm. The energy band gap of as synthesized Mn doped Cu₂O is calculated as 4.4, 4.5, 4.6, 4.7 eV respectively. This shows that, the band gap increased as the concentration was increased and the wavelength shifts towards the lower value. A blue shift of the absorption edge is exhibited for all samples.

V. Electrical Properties

Electrical properties of Mn (4% & 8%) doped cuprous oxide nanoparticles were studied using impedance spectroscopy. Various electrical parameters like dielectric constant, real and imaginary components of impedance were measured over a wide range of frequency for the samples.

5.1. Dielectric Properties:

The complex dielectric permittivity $\epsilon^* = \epsilon' - i\epsilon''$ of Mn doped Cu₂O nanoparticles was measured as a function of frequency, where ϵ' is real part of dielectric constant and describes the stored energy while ϵ'' is imaginary part of dielectric constant, which describes the dissipated energy. The dielectric constants as a function of frequency are shown in Fig 6. The dielectric constant decreases with the increase in frequency and become almost constant at high frequencies [19].

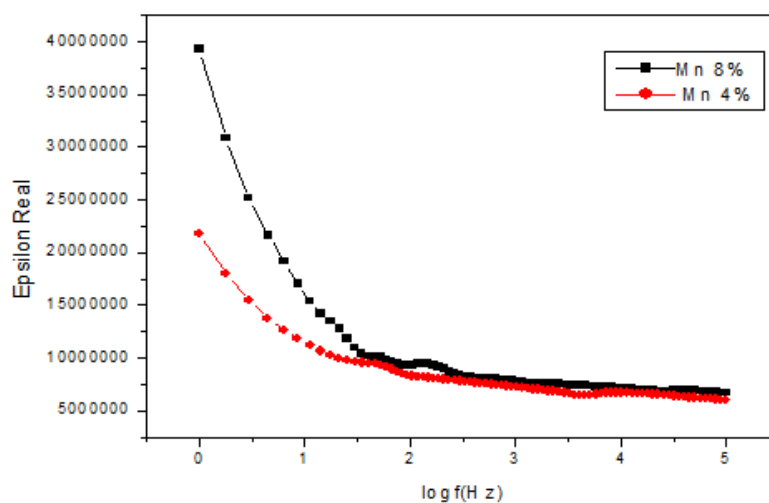


Figure 6. Variation in dielectric constant (ϵ') with frequency

This can be attributed to the fact that at low frequencies, the hopping plays in unison with the applied ac field, but at the elevated frequencies, the hopping ceases to follow the rapid fluctuation of the field and hence

ϵ' decreases due to random orientation and chaotic dipolar distribution up to certain frequency and show the frequency independent behaviour at higher frequencies.

5.2. Impedance Analysis:

The total impedance of any system is given by $Z = Z' + Z''$, where Z' is the real part of impedance which is related to a pure resistance R , Z'' is the imaginary part of impedance that can be related to a capacitor C . Figure 8(a) and 8(b) show the variation of the real (Z') and imaginary (Z'') parts, where the values are high in the low frequency region. This effect is due to the accumulation of free charges at the pellet –electrolyte interface. All the curves merge in high-frequency region and then become independent of frequency. Such behaviour indicates the presence of relaxation in the system.

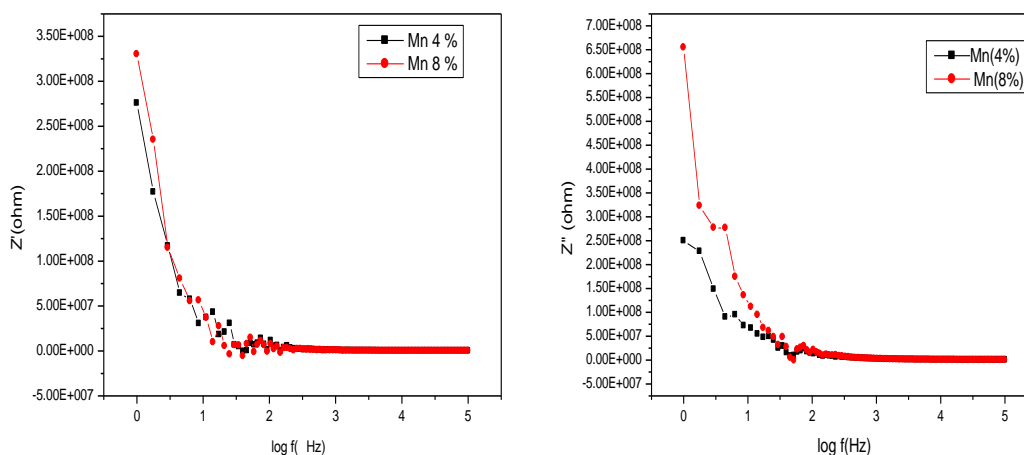


Figure 8 (a) & (b). Variation of real and imaginary impedance with frequency and composition

VI. Conclusion

Pure and Mn doped Cu_2O nanoparticles having crystallite diameters 41~33 nm were obtained by a simple solvothermal microwave method. By FTIR spectra we confirmed the purity of the prepared samples. SEM results were consistent with the previous XRD results. The doping levels and the bonding characteristics have been determined by EDAX spectrum. This also shows that Mn^{2+} impurity has entered in the crystal matrix of Cu_2O . All the samples showed a blueshift in the optical band gap, which can be assigned to the quantum confinement effects. Complex impedance analysis was used to distinguish the grain boundary contributions to the system, suggesting the dominance of grain boundary resistance in the synthesized samples. The dielectric constant and dielectric loss were studied as a function of frequency. They show the general decreasing trend with the increase in frequency for both pure and doped samples.

Acknowledgement

I sincerely express my profound gratitude to my guide Dr. S. John kennadyvethanathan for his excellent guidance, encouragement, suggestions and timely advices for the implementation of this work. I thank my family members and friends for their kindly help and continuous support.

References

- [1]. Liang Y Q, Gao Z H, Cui Z D, Zhu S L, Li Z Y, Yang X J (2014), Photo catalytic performance of Ag nanoparticles modified ZnO micro plates prepared by one-step method. *Curr.nanosci.*10 (3), 389-393.
- [2]. Rajabi A R, Jabbarzare S, Mohammad shafiee M R, Ghashang M (2014), Barium doped ZnO nanoparticles: Preparation and evaluation of their catalytic activity, *Curr. Nanosci* 10(2), 312-317.
- [3]. Han S, Hu L, Gao N, Al-Ghamdi A A, Fang X, (2014) Efficient self assembly synthesis of uniform CdS spherical nanoparticles- Au nanoparticles hybrids with enhanced photoactivity, *Adv.Funct.Mater.*24(24),3725-3733.
- [4]. Liu H, Hu L, Watanabe K, Hu X, Dierre B, Kim B, Sekiguchi T, Fang X, (2013), Cathode luminescence modulation of ZnS nanostructures by morphology, Doping and Temperature, *Adv. Funct. Mater.* 23(29), 3701-3709.
- [5]. Motogoshi R, Oku T, Suzuki A, Kikuchi K, Kihuch S, Jeyadwan B and Cuya J, (2010), Fabrication and characterization of cuprous oxide fullerene solar cells, *Synthetic metals*, 160,11-12. ChLi, Yin Y, Hou H, Fan N, Yuan F, Shi Y, Meng Q, (2010), *Solid state commun.* 150 (585).
- [6]. Topnani N, Kushwaha S, Athar T, (2009), *Int. J.Green nanotechnology, Mater. Sci. Eng.* 67.
- [7]. Salavati-Niasari M. Davar F, (2009), *Mater let.* 63,441.
- [8]. Ying J, Li, sh, Xiog B, Xi X G, Li Y, Qian T (2009), *Cryst. Growth Des.* 9, 4108.

- [9]. Shang D, Yua K, Zhang Y, Xu J, Wu J, Xu Y, Li L, Zhu Z, (2009), *Appl. Surface Sci.*, 225, 4093.
- [10]. Wua R, Maa Z, Gua Z, Yang Y, (2010), *Alloys. Comp.*, 504, 45.
- [11]. Zhou K, Wang R, Xu B, Li L, (2006), *Nanotechnology*, 17, 3939.
- [12]. Kalchuck N S, Strizhak P E, Kosmambetova G R, Didenko O Z, (2008), *Theor. Exp. Chem*, 44, 172.
- [13]. Zhang X, Zhang D, Ni X, Zheng H, (2008), *Solid state electron*, 52, 245.
- [14]. Rejith S G and Krishnan C, (2013), *Advances in applied science research*, 4(2), 103-109.
- [15]. Volanti D P et al, (2008), *Journal of alloys and compounds (Elsevier)*, 459, 537-542.
- [16]. Ponnarasan V, Krishnan A, (2014), *Adv. Studies. Theor. phys.*, 8(6), 251-258.
- [17]. Agekyan V T, (1977), *phys. status solids A*43, 11.
- [18]. AmeerAzam, Arham, Ahmed S, Chaman M, (2010), *Journal of applied physics*, 108.